Theor. Appl. Climatol. 67, 135–151 (2000)

Theoretical and Applied Climatology

[1] Faculty of Agriculture, University of Novi Sad, Novi Sad, Yugoslavia
[2] Science Applications International Inc., McLean, VA, USA
[3] Department of Atmospheric Science, Colorado State University, Fort Collins, CO, USA
[4] Faculty of Physics, University of Belgrade, Belgrade, Yugoslavia
[5] Klimaforschung ETH/Climate Research ETH, Zurich, Switzerland

Comparison of different boundary layer surface schemes using single point micrometeorological field data

D. T. Mihailović[1], **T. J. Lee**[2], **R. A. Pielke**[3], **B. Lalić**[1], **I. D. Arsenić**[1], **B. Rajković**[4], and **P. L. Vidale**[5]

With 6 Figures

Received November 23, 1999
Revised August 18, 2000

Summary

In the last decade, a vast number of land surface schemes has been designed for use in global climate models, atmospheric weather prediction, mesoscale numerical models, ecological models, and models of global changes. Since land surface schemes are designed for different purposes they have various levels of complexity in the treatment of bare soil processes, vegetation, and soil water movement.

This paper is a contribution to a little group of papers dealing with intercomparison of differently designed and oriented land surface schemes. For that purpose we have chosen three schemes for classification: i) global climate models, BATS (Dickinson et al., 1986; Dickinson et al., 1992); ii) mesoscale and ecological models, LEAF (Lee, 1992) and iii) mesoscale models, LAPS (Mihailović, 1996; Mihailović and Kallos, 1997; Mihailović et al., 1999) according to the Shao et al. (1995) classification. These schemes were compared using surface fluxes and leaf temperature outputs obtained by time integrations of data sets derived from the micrometeorological measurements above a maize field at an experimental site in De Sinderhoeve (The Netherlands) for 18 August, 8 September, and 4 October 1988. Finally, comparison of the schemes was supported applying a simple statistical analysis on the surface flux outputs.

1. Introduction

The modelling of heat, mass, and momentum exchanges between the air and different types of surfaces is important for the correct feedbacks between atmospheric, hydrological, and ecological models. As a result of this need, a number of land surface schemes have been designed starting from the pioneering work of Manabe (1969). The designed schemes have been based on a variety of concepts with different levels of complexity. The major goal of these models is to represent the most important physical and biochemical aspects of land surface processes which are relevant for the feedback between the models. The current state that future plans in this field are comprehensively described in papers by Henderson-Sellers et al. (1993) and Chen T. H. et al. (1997).

The form of the feedback models depends on the spatial and temporal scale of the atmospheric, hydrological (Lohmann et al., 1996; Mihailović et al., 1998; Mihailović et al., 1999), and ecological models. For example, for global climate models it is essential to correctly parameterize the energy and momentum transport from the surface on hourly to annual and longer time scales and on a spatial scale corresponding to the GCM grid structure. On the other hand, numerical weather prediction and mesoscale models are designed in order to correctly parameterize processes on hourly and daily scales, with spatial scales corresponding to the higher resolution of those models (Betts et al., 1997; Chen F. Z. et al., 1997). In contrast, ecological models, which focus on carbon storage, tend to precisely simulate the annual cycle of soil moisture and ignore the parameterization of hourly surface energy and momentum fluxes.

A number of existing land surface schemes have, therefore, been developed for different purposes. Thus there is the question of the procedure to compare them with observations and to other schemes. The appropriate comparison is crucial to their verification and acceptance. As indicated above, the time scale problem is an important issue in comparing and evaluating land surface schemes. According to Shao et al. (1995) the two most important time scales in land surface processes are reflected in diurnal changes of surface energy fluxes, photosynthetic activities of the plants, surface temperature and soil moisture in the upper soil layers, and in the annual changes of these.

The present paper is a contribution to a group of papers with respect to interscheme comparisons (e.g., Vogel et al., 1995; Chen T. H. et al., 1997). The basic idea is to investigate how several differently designed land surface schemes reproduce the diurnal evolution of latent and sensible heat fluxes and leaf temperature using micrometeorological data sets over maize for validation. We have chosen three schemes for this study: i) the Biosphere-Atmosphere Transfer Scheme, BATS (Dickinson et al., 1986; Dickinson et al., 1992); ii) Land Ecosystem-Atmosphere Feedback model, LEAF (Lee, 1992); and iii) the Land Air Parameterization Scheme, LAPS (Mihailović et al., 1993; Mihailović, 1996; Mihailović and Ruml, 1996; Mihailović et al., 1997; Mihailović and Kallos, 1997). A concise description of the considered schemes is presented in Section 2. Section 3 contains the information on soil, plant, and micrometeorological measurements above a maize field at an experimental site at De Sinderhoeve (The Netherlands) for 18 August, 8 september and 4 October, 1988. The latent and sensible heat fluxes and canopy temperature outputs obtained from the time integrations for the three schemes are presented in Section 4. A comparison of the schemes using statistical analysis and a discussion of the results are also included in this section.

2. Model description

The basic equations for the three surface-vegetation transfer schemes (SVATS) used in the calculation of surface fluxes of heat and water, and the hydrological modules used in the intercomparisons are summarized in Tables 1 to 4, with the intent of providing easy access to basic differences in model physics and formulation.

In these tables we have provided a basic framework for comparison of the SVATS, though model structures are somewhat dissimilar (e.g., LEAF has multiple soil layers, BATS and LAPS have 2 and 3, respectively). The references for the specific version of the SVATS schemes used in this study were Mihailović (1990) for BATS and the foregoing indicated references for LAPS and LEAF.

3. Data used in runs for comparison

For the comparison of the chosen land surface schemes, we used a data set which is a part of a larger measurement program which examined the exchange processes of heat, mass, and momentum just above and within a maize canopy during its growing season in De Sinderhoeve (The Netherlands). The experimental site was in the center of the Netherlands (51° 59′ N, 5° 45′ E). The site was 250 m × 300 m, surrounded by other agricultural fields where maize is dominant. The maize was planted in north-northeast/south-southwest rows with a row spacing of 0.75 m and with 0.11 m spacing in the row (12 plants per m^2). We selected three situations that represented the maize in different growth stages: 18 August, 8 September, and 4 October. These are denoted as MA, MS, and MO, respectively. These data sets were selected because they covered a wide range of fractional covers and leaf-area index (LAI; one-sided leaf area per unit ground surface). These parameters, together with the maize height, the roughness length, and the displacement height were measured (Jacobs et al., 1990; van Pul, 1992). The minimum stomatal resistance was not measured and was assumed to be equal to 200 s m^{-1}. The texture of soil at the experimental

Table 1. Basic equations for BATS, LAPS, and LEAF prognostic equations

a. Canopy, ground surface, and deep soil temperature (T_f, T_g, and T_d, respectively)

	BATS	LAPS	LEAF
Canopy	$R_f^{net}(T_f) - H_f(T_f) - \lambda E_f(T_f) = 0$	$C_f \frac{\partial T_f}{\partial t} = R_f^{net} - H_f - \lambda E_f$	$C_f \frac{\partial T_f}{\partial t} = R_f^{net} - H_f - \lambda E_f$
Soil Surface	$\frac{\partial T_g}{\partial t} = \frac{(2\pi)^{1/2}}{\rho_s C_s (K_s \tau_d)^{1/2}} [R_g^{net} - H_g - \lambda E_g]$	$C_g \frac{\partial T_f}{\partial t} = R_g^{net} - H_g - \lambda E_g - G$	$C_g \frac{\partial T_g}{\partial t} = R_g^{net} - H_g - \lambda E_g - G$
Deep soil	$\frac{\partial T_d}{\partial t} = -0.2 \left[\frac{T_d - T_g}{\tau_d} + c(T_d - \bar{T}) + Q_g \right]$	$C_g \frac{\partial T_d}{\partial t} = \frac{2(R_g^{net} - H_g - \lambda E_g)}{(365\pi)^{1/2}}$ $C_g = 0.95[\lambda_H C_v/(2\omega)]^{1/2}$	$\lambda_H = \exp(-(P_f + 2.7)) \quad P_f \leq 5.1$ $\lambda_H = 0.00041 \quad P_f > 5.1$ $C_g \frac{\partial T_i}{\partial t} = \frac{\partial}{\partial z}\left(\lambda_H \frac{\partial T_i}{\partial z}\right) \quad C_g = (1 - \eta_s)C_i + \eta$

where 1,2,... d =soil level (1 superficial, 2 or i intermediate layers, 3 or d is the deepest layer; LEAF has multiple soil layers)

c = damping of soil surface temperature to annual value (s^{-1})
C_g, C_f = effective heat capacities ($J\,m^{-2}\,K^{-1}$)
C_i = air dry volumetric heat capacity for soil type ($J\,m^{-3}\,K^{-1}$)
C_s = specific heat of subsurface layer per unit mass ($J\,kg^{-1}\,K^{-1}$)
C_v = volumetric soil heat capacity ($J\,m^{-3}\,K^{-1}$)
E_g, E_f = evaporatioin and evapotranspiration rates ($kg\,m^{-2}\,s^{-1}$)
G = soil heat flux ($W\,m^{-2}$)
H_g, H_f = sensible heat flux from the soil surface (g) and canopy (f) ($W\,m^{-2}$)
K_s = thermal conductivity ($m^2\,s^{-1}$)
P_f = the base 10 logarithm of moisture potential Ψ expressed in cm
Q_g = rate of subsoil temperature change because of melting or freezing ($K\,s^{-1}$)
R_g^{net}, R_f^{net} = net radiation absorbed by the soil surface (g) and canopy (f) ($W\,m^{-2}$)
$\bar{T}$ = fixed annual mean deep soil temperature (K)
T_f, T_g, T_d = temperature of the canopy (f), soil surface (g) and deep soil (d) (K)
T_i = temperature of ith soil layer (K)
η = volumetric moisture content ($m^3\,m^{-3}$)
η_s = saturation moisture content ($m^3\,m^{-3}$)
λ = latent heat of vaporization ($J\,kg^{-1}$)
λ_H = thermal conductivity ($J\,s^{-1}\,m^{-1}\,K^{-1}$)
ρ_s = soil density ($kg\,m^{-3}$)
τ_d = daylength (s)
$\omega = 2\pi/\gamma_d$

b. Interception stores

	BATS	LAPS	LEAF
Canopy	$\frac{\partial w_f}{\partial t} = \sigma_f P - (E_{wf} - E_t)/\rho_w$	$\frac{\partial w_f}{\partial t} = P - \frac{E_{wf}}{\rho_w}$	$\frac{\partial w_f}{\partial t} = P - \frac{E_{wf}}{\rho_w}$

where E_t = transpiration rate from the dry fraction of the leaves ($kg\,m^{-2}\,s^{-1}$)

E_{wf} = evaporation from interception stores ($kg\,m^{-2}\,s^{-1}$)
P = precipitation reaching the leaves ($m\,s^{-1}$)
w_f = water stored on the canopy (m)
ρ_w = density of water ($kg\,m^{-3}$)
σ_f = vegetation fractional cover

Table 1 (continued)
c. Soil moisture stores

	BATS	LAPS	LEAF
Surface layer	$\frac{\partial S_{sw}}{\partial t} = \Gamma - R_s + \gamma_{w1}$	$\frac{\partial w_1}{\partial t} = \frac{1}{D_1}\left[P - Q_{1,2} - \frac{E_g + E_{t1}}{\rho_w} - R_s - R_1\right]$	$\frac{\partial w_1}{\partial t} = \frac{1}{D_1}\left[P - Q_{1,2} - \frac{E_g + E_{t1}}{\rho_w} - R_s\right]$
	$\frac{\partial S_{rw}}{\partial t} = \Gamma - R_s + \gamma_{w2}$	$\frac{\partial w_2}{\partial t} = \frac{1}{D_2}\left[Q_{1,2} - Q_{2,3} - \frac{E_{t2}}{\rho_w} - R_2\right]$	$\frac{\partial w_{gi}}{\partial t} = \frac{1}{D_i}\left[Q_{i-1,i} - Q_{i+1,i} - \frac{E_{ti}}{\rho_w}\right]$
Deep layer	$\frac{\partial S_{tw}}{\partial t} = \Gamma - R_s - R_g$	$\frac{\partial w_3}{\partial t} = \frac{1}{D_3}[Q_{2,3} - Q_g - R_3]$	$\frac{\partial w_{gd}}{\partial t} = \frac{1}{D_d}\left(Q_{d-1,d} - \frac{E_{td}}{\rho_w}\right)$
	$\Gamma = P + S_m - E_f$		

where 1,2,… d = soil level (1 superficial, 2 or i intermediate layers, 3 or d is the deepest layer; LEAF has multiple soil layers)
D_i = thickness of the ith soil layer (m)
E_{ti} = water extracted from the ith layer by transpiration $(\mathrm{m\,s^{-1}})$
P = infiltration of precipitation into the upper soil moisture store $(\mathrm{m\,s^{-1}})$
Q_g = gravitational drainage $(\mathrm{m\,s^{-1}})$
$Q_{i,i+1}$ = flow between i and $i+1$ layers $(\mathrm{m\,s^{-1}})$
R_i = subsurface runoff in ith soil layer $(\mathrm{m\,s^{-1}})$
R_s = surface runoff $(\mathrm{m\,s^{-1}})$
R_g = leakage down to subsoil and groundwater reservoirs $(\mathrm{m\,s^{-1}})$
S_m = snow melt (m)
S_{sw} = surface soil water representing water in upper layer of soil (m)
S_{rw} = water in rooting zone of soil (m)
S_{tw} = total water in the soil to selected depth (m)
w_l = volumetric soil moisture content for ith larger
γ_{wi} = rate of transfer of water to the upper soil layer from the lower $(\mathrm{m\,s^{-1}})$

Table 2. Surface fluxes for BATS, LAPS and LEAF schemes
a. Fluxes from ground surface to canopy air space

	BATS	LAPS	LEAF
Evaporation rate	$E_g = \rho\beta_w C_D U_r[(1-\sigma_f) + C_D^{1/2}\sigma_f]\cdot(q_g^s - q_{af})$	$E_g = \frac{\rho c_p}{\gamma\lambda}\frac{\alpha_m e_g^s - e_{af}}{r_l + r_d}(1-\sigma_f)$	$E_g = \rho\frac{q_{af} - q_g}{r_d}$
Sensible heat flux	$H_g = \rho c_p C_D U_r[(1-\sigma_f) + C_D^{1/2}\sigma_f]\cdot(T_g - T_{af})$	$H_g = \rho c_p\frac{T_g - T_{af}}{r_d}$	$H_g = \rho c_p\frac{T_{af} - T_g}{r_d}$

where C_D = drag coefficient
c_p = specific heat of air at constant pressure $(\mathrm{J\,K^{-1}\,kg^{-1}})$
e_{af} = vapor pressure within the canopy (mb)
e_g^s = saturated vapor pressure at ground surface temperature (mb)
q_{af} = specific humidity within the canopy $(\mathrm{kg\,kg^{-1}})$
q_g = specific humidity immediately above the surface $(\mathrm{kg\,kg^{-1}})$
q_g^s = saturated specific humidity at ground surface temperature $(\mathrm{kg\,kg^{-1}})$
r_d = aerodynamic resistance between the ground and the canopy air space $(\mathrm{s\,m^{-1}})$
r_l = bare soil surface resistance $(\mathrm{s\,m^{-1}})$
T_{af} = air temperature within the canopy (K)
U_r = wind speed at refernce level $(\mathrm{m\,s^{-1}})$
α_m = wetness factor (see Mihailović et al., 1993)
β_w = wetness factor (see Dickinson, 1986)
γ = psychrometric constant $(\mathrm{mb\,K^{-1}})$
ρ = air density $(\mathrm{kg\,m^{-3}})$

Table 2 (continued)

b. Fluxes from foliage to canopy air space

	BATS	LAPS	LEAF
Evaporation from interception stores	$E_{wf} = \rho \dfrac{(q_f^s - q_{af})}{r_b}$	$E_{wf} = \dfrac{\rho c_p}{\gamma\lambda} \dfrac{e_f^s - e_{af}}{r_b} \left(\dfrac{w_f}{w_m}\right)^{2/3}$	$E_{wf} = \rho \dfrac{q_{af} - q_f^s}{r_b} \left(\dfrac{w_f}{w_m}\right)^{2/3}$
Transpiration rates	$E_t = H_w(E_{wf}) \left[1 - \left(\dfrac{w_f}{w_m}\right)^{2/3}\right] \dfrac{\text{LAI}}{\text{SAI}} \dfrac{r_b}{r_b + r_c} E_{wf}$	$E_t = \dfrac{\rho c_p}{\gamma\lambda} \dfrac{e_f^s - e_{af}}{r_b + r_c} \left(1 - \dfrac{w_f}{w_m}\right)^{2/3}$	$E_t = \rho \dfrac{q_{af} - q_f^s}{r_b + r_c} \left(1 - \dfrac{w_f}{w_m}\right)^{2/3}$
Evapotranspiration rate	$E_f = r'' E_{wf}$ $r'' = 1 - H_w(E_{wf}) \left\{1 - \left(\dfrac{w_f}{w_m}\right)^{2/3} - \left[1 - \left(\dfrac{w_f}{w_m}\right)^{2/3}\right] \dfrac{\text{LAI}}{\text{SAI}} \dfrac{r_b}{r_c + r_b}\right\}$	$E_f = \dfrac{\rho c_p}{\gamma\lambda} (e_f^s - e_{af}) \cdot \left[\dfrac{\left(\dfrac{w_f}{w_m}\right)^{2/3}}{r_b} + \dfrac{1 - \left(\dfrac{w_f}{w_m}\right)^{2/3}}{r_b + r_c}\right]$	$E_f = \rho (q_{af} - q_f^s) \cdot \left[\dfrac{\left(\dfrac{w_f}{w_m}\right)^{2/3}}{r_b} + \dfrac{1 - \left(\dfrac{w_f}{w_m}\right)^{2/3}}{r_b + r_c}\right]$
Sensible heat flux	$H_f = \sigma_f \text{SAI} \rho c_p \dfrac{T_f - T_{af}}{r_b}$	$H_f = \rho c_p \dfrac{T_f - T_{af}}{r_b}$	$H_f = \rho c_p \dfrac{T_f - T_{af}}{r_b}$

where LAI = leaf area index $(\text{m}^2\,\text{m}^{-2})$
e_f^s = saturated vapor pressure at canopy temperature (hPa)
q_f^s = saturated specific humidity at canopy temperature $(\text{kg}\,\text{kg}^{-1})$
r_b = bulk leaf boundary layer resistance $(\text{s}\,\text{m}^{-1})$
r_c = canopy resistance $(\text{s}\,\text{m}^{-1})$
w_m = maximum water reservoir depth (m)
SAI = stem area index $(\text{m}^2\,\text{m}^{-2})$
H_w = a step function and is one for positive argument and zero for negative argument

c. Fluxese from ground surface and foliage to the atmosphere

	BATS	LAPS	LEAF
Evaporation rate	$E_f = \rho C_D U_r \cdot (q_{af} - q_r)$	$E_f = \dfrac{\rho c_p}{\gamma\lambda} \dfrac{e_{af} - e_r}{r_a}$	$E_f = \rho \dfrac{q_r - q_{af}}{r_a}$
Sensible heat flux	$H_t = \rho c_p C_D U_r \cdot (T_{af} - T_r)$	$H_t = \rho c_p \dfrac{T_{af} - T_r}{r_a}$	$H_t = \rho c_p \dfrac{T_r - T_{af}}{r_a}$

where e_r = vapor pressure at reference height (hPa)
q_r = specific humidity at reference height $(\text{kg}\,\text{kg}^{-1})$
r_a = aerodynamic resistance $(\text{s}\,\text{m}^{-1})$
T_r = air temperature at reference height (K)

Table 3. Resistances used in flux calculations in BATS, LAPS and LEAF schemes.

a. Aerodynamic resistance

BATS	LAPS	LEAF
$r_a = \dfrac{1}{C_D(R_{iB})U_r^{1/2}}$	$r_a = \dfrac{1}{ku_*}\ln\dfrac{z_r - d}{H - d}$	$r_a = \dfrac{1}{k^2 U_r}\left(\ln\dfrac{z_r - d}{z_0} + \Psi_M\right)\cdot\left(\ln\dfrac{z_r - d}{z_0} + \Psi_H\right)$

where d = zero plane displacement height (m)
H = canopy height (m)
k = von Karman's constant
R_{iB} = surface bulk Richardson number
u_* = friction velocity $(\mathrm{m\,s^{-1}})$
z_r = reference height (m)
z_0 = roughness length (m)
Ψ_H = stability function for moisture transfer
Ψ_M = stability function for momentum transfer

b. Soil surface resistance

BATS	LAPS	LEAF
not used	$r_d = \dfrac{1}{k^2 u_H}\left[\dfrac{\mathrm{sh}(\beta)}{\mathrm{sh}(\alpha_g\beta)}\right]^{1/2}\ln^2\left(\dfrac{z}{z_0}\right)$	$r_d = r_{\mathrm{bare}}\max\left[\left(1 - \dfrac{\mathrm{LSAI}}{\sigma_f}\right), 0\right] + r_{\mathrm{close}}\min\left[\dfrac{\mathrm{LSAI}}{\sigma_f}, 1\right]$

where LSAI = leaf and stem area index
r_{bare} = resistance when the surface is bare (see Lee et al., 1992) $(\mathrm{s\,m^{-1}})$
r_{close} = resistance when the surface is covered by a closed canopy (see Lee et al., 1992) $(\mathrm{s\,m^{-1}})$
u_H = wind speed at canopy top height $(\mathrm{m\,s^{-1}})$
α_g = ratio of canopy bottom height and canopy top height
β = extinction factor (see Lee et al., 1992)

c. Bulk leaf boundary layer resistance

BATS	LAPS	LEAF
$r_b = \dfrac{1}{C_f}\left(\dfrac{1}{U_f}\right)^{1/2}$	$r_b = \dfrac{(\mathrm{sh}\beta)^{1/4}}{(u_H)^{1/2}L_d H}\cdot\displaystyle\int_{\alpha_g\beta}^{\beta}\left[\mathrm{sh}\left(\dfrac{\beta z}{h}\right)\right]d\left(\dfrac{\beta z}{H}\right)$	$r_b = \dfrac{P_s}{C_f\mathrm{LSAI}}\left(\dfrac{L}{U_f}\right)^{1/2}$ $P_s = 1 + 0.5\mathrm{LSAI}$

where $C_f = 0.01\,\mathrm{m\,s^{-1/2}}$ constant after Gates (1980)
U_f = magnitude of wind within the canopy $(\mathrm{s\,m^{-1}})$
L = dimension of leaves or the stems along the wind directions (m)
L_d = stem and leaf density $(\mathrm{m^{-2}\,m^3})$
P_s = shelter factor

d. Surface resistance

BATS	LAPS	LEAF
not used	$r_1 = p_1 + p_2\left(\dfrac{w_1}{w_s}\right)^{p_3}$	not used

where $p_1, p_2, p_3 = 30\,\mathrm{s\,m^{-1}}$, 3.5, 2.3 empirical constants, respectively (see Mihailović and Ruml, 1996)
w_s = saturated values of volumetric soil moisture content in the top soil layer $(\mathrm{m^3\,m^{-3}})$

e. Canopy resistance

BATS	LAPS	LEAF
$r_c = \dfrac{r_{s\min}}{\mathrm{LAI}} f_R f_T f_s f_v$	$r_c = \dfrac{r_{s\min}}{\mathrm{LAI}} f_R[f_v f_T f_w]^{-1}$	$r_c = \dfrac{1}{\mathrm{LAI}}[d_{s\min} + (d_{s\max} + d_{s\min})\cdot f_R f_{T_c} f_{T_h} f_v f_\Psi]^{-1}$

where $d_{s\min}$ = minimum stomatal conductance $(\mathrm{m\,s^{-1}})$
$d_{s\max}$ = maximum stomatal conductance $(\mathrm{m\,s^{-1}})$
f_R = adjustment factor for total solar radiation
f_s = adjustment factor for soil moisture
f_T = adjustment factor for seasonal air temperature changes
f_{T_c} = adjustment factor for leaf temperature at cold range
f_{T_h} = adjustment factor for leaf temperature at hot range
f_v = adjustment factor for water vapor pressure deficit
f_w = adjustment factor for soil moisture
f_Ψ = adjustment factor for soil water potential
$r_{s\min}$ = minimum stomatal resistance $(\mathrm{m\,s^{-1}})$

Table 3 (continued)
f. Adjustment factor

$$f_R = \left[1 + \frac{1.1S/S_g}{\text{LAI}}\right]\left[\frac{1.1S/S_g}{\text{LAI}} + \frac{r_{s\,\min}}{r_{s\,\max}}\right]^{-1}$$

$$f_T = 1 - 0.0016(298.0 - T_{af})^2$$

f_s = (see Dickinson et al., 1986, pp. 48–51)

$$f_v = 1\text{–}0.0025\,\text{hPa}^{-1}\;[e_s(T_f)\text{–}e_{af}]$$

$$f_w = \begin{cases} 1 & w_a > w_{fc} \\ 1 - \left[\dfrac{w_{\text{wil}}}{w_a}\right]^{1.5} & w_{\text{wil}} \le w_a \le w_{fc} \\ & w_a < w_{\text{wil}} \end{cases}$$

f_{Tc}, f_{Th}, f_{Ψ} = (see Lee at al., 1992)

where S = incoming shortwave solar radiation (W m^{-2})
S_g = the limit value of $30\,\text{W m}^{-2}$ for a forest and $100\,\text{W m}^{-2}$ for crops
w_a = mean volumetric soil moisture content in the first and second layer ($\text{m}^3\,\text{m}^{-3}$)
w_{fc} = volumetric soil moisture content at field capacity ($\text{m}^3\,\text{m}^{-3}$)
w_{wil} = volumetric soil moisture content at wilting point ($\text{m}^3\,\text{m}^{-3}$)
$r_{s\,\max}$ = maximum stomatal resistance (s m^{-1})

site was very similar to soil texture indicated in a paper by Jacobs et al. (1990). The maize and soil parameters used in the runs are listed in Table 5 and Table 6, respectively. Other parameters used in the tests can be found in Mihailović (1990), Dickinson et al. (1986), Mihailović et al. (1992) and Mihailović and Ruml (1996).

The MA and MS cases correspond to the periods of the growing season when the maize plants were tall (2.20 and 2.30 m). As a result, the values of LAI and fractional cover σ_f increased significantly. During these days, the wind speed at the reference height U_r varied between $0.4\,\text{m s}^{-1}$ and $1.2\,\text{m s}^{-1}$ at night, and $3.28\,\text{m s}^{-1}$ and $3.83\,\text{m s}^{-1}$ in the afternoon for the MA and MS cases, respectively. The maximum incoming shortwave radiation was $636\,\text{W m}^{-2}$ for MA and $604\,\text{W m}^{-2}$ for MS case. The MO case was already at the end of the growing season and a substantial fraction of the bare soil was visible ($\sigma_f = 0.50$). The incoming shortwave radiation was considerably reduced so that the maximum reached just $409\,\text{W m}^{-2}$.

The atmospheric boundary conditions at the reference level, $z_r = 4.5\,\text{m}$, were derived from measurements of global radiation, cloudiness, precipitation, specific humidity, temperature and average wind speed for 24 h from 000 LST at 15-min intervals. These values were interpolated to the beginning of each time step ($\Delta t = 600\,\text{s}$). All time integrations were started at 0000 LST with the initial values of atmospheric pressure of 1016 hPa (MA), 1024 hPa (MS), and 1016 hPa (MO). The initial value of volumetric soil moisture content and soil surface temperature were derived from Mihailović (1990).

4. Results of comparison and discussion

The comparison of the land surface schemes will start by analyzing the one-day time integration of surface flux outputs. Figures 1 to 3 show the diurnal variations of the computed surface energy components for the three chosen situations. The observed values of the latent and sensible heat fluxes for the MA, MS, and MO cases are indicated by black and white squares, respectively. These values were obtained from van Pul (1992).

Looking at panels in Fig. 1 it can be seen that different levels of the agreement with the observations for the MA case were achieved by the above schemes. BATS more correctly simulates the latent heat flux around noon than the other schemes. For the period indicated, LAPS completely underestimates the measured values while LEAF shows a weak tendency to overestimate them. The latent heat flux values modeled by BATS lie between the two other schemes.

These differences can be addressed to the different approaches in the concept of the transpiration in the considered schemes. Namely, the processes and mechanisms controlling transpiration are complicated, involving the interaction of environmental factors radiation, ambiental temperature, soil properties and biological (water extraction by root, transport water through the tissue, stomatal activities). Thus, in order to numerically represent the interaction of biotic and abiotic factors, some simplification was introduced. The different level of simplification in the schemes determined different stomatal resistance values and consequently different amounts of transpired water were simulated. The schemes show quite different behaviors for the period between noon and the early evening hours. The worst agreement with observations is for LEAF while BATS much better reproduces this part of the daily trend. Careful inspection demonstrates

Table 4. Hydrology in BATS, LAPS and LEAF schemes

a. Vertical movement of water through soil

	BATS	LAPS	LEAF
Vertical water flux	$Q_{i,i+1} = K_s B\left(\frac{w_i}{w_s}\right)^{2B+3}$	$Q_{i,i+1} = \frac{D_i K_i + D_{i+1} K_{i+1}}{D_i + D_{i+1}}\left[\frac{2(\Psi_i - \Psi_{i+1})}{D_i + D_{i+1}} + 1\right]$	$Q_{i,i+1} = -K_i \frac{d}{dz}(\Psi_i + z)$
Hydraulic conductivity	$K_i = K_s\left(\frac{w_i}{w_s}\right)^{2B+3}$	$K_i = K_{si}\left(\frac{w_i}{w_s}\right)^{2B+3}$	$K_i = K_s\left(\frac{w_i}{w_s}\right)^{2B+3}$
Soil water potential	$\Psi_i = \Psi_s\left(\frac{w_i}{w_s}\right)^{-B}$	$\Psi_i = \Psi_s\left(\frac{w_i}{w_s}\right)^{-B}$	$\Psi_i = \Psi_s\left(\frac{w_i}{w_s}\right)^{-B}$
Gravitational drainage	$R_g = K_s\left(\frac{w_2}{w_s}\right)^{2B+3}$	$R_g = K_s\left(\frac{w_3}{w_s}\right)^{2B+3} \sin x$	$\frac{\partial}{\partial t}(w_d) = 0$

where 1,2,... d = soil level (1 superficial, 2 or i intermediate layers, 3 or d is the deepest layer; LEAF has multiple soil layers)
B = Clapp Hornberger constant
D_i = thickness of ith layer (m)
K_i = hydraulic conductivity of ith layer $(\mathrm{m\,s^{-1}})$
K_s = saturated hydraulic conductivity $(\mathrm{m\,s^{-1}})$
w_d = volumetric soil moisture content of the deep layer $(\mathrm{m^3\,m^{-3}})$
w_i = volumetric soil moisture content of the ith layer $(\mathrm{m^3\,m^{-3}})$
w_s = saturated volumetric soil moisture content $(\mathrm{m^3\,m^{-3}})$
x = mean slope angle (°)
z = vertical coordinate (m)
Ψ_i = soil water potential (m)
Ψ_s = saturated soil water potential (m)

b. Horizontal movement of water in the soil

	BATS	LAPS	LEAF
Surface runoff	$R_s = \left[\frac{s_1 + s_0}{2}\right]^4 \left(P + S_m - \frac{E_f}{\rho_w}\right)$	$R_s = P_1 - \min(P_1, K_s)$	$R_s = P_1 - \min(P_1, K_s)$
Subsurface runoff	not used	$R_i = Q_i - \min(Q_{i,i+1}, K_s)$	not used in Version 1

where $s_0 = w_0/w_s$ for the depth of the soil active layer (see Dickinson et al., 1986)
$s_1 = w_1/w_s$ in the upper soil layer
P_1 = infiltration rate into the soil $(\mathrm{m\,s^{-1}})$

Table 5. Soil parameters at test site De Sinderhoeve (The Netherlands)

Parameter	Symbol	Unit	Value
Volumetric soil moisture content at field capacity	w_{fc}	$m^3\,m^{-3}$	0.15
Volumetric soil moisture content at saturation	w_s	$m^3\,m^{-3}$	0.41
Wilting point volumetric soil moisture content	w_{wil}	$m^3\,m^{-3}$	0.075
Clapp Hornberger constant	B		4.38
Heat capacity of solid soil fraction	C_s	$J\,kg^{-1}\,K^{-1}$	820
Saturated hydraulic conductivity	K_s	$m\,s^{-1}$	$0.95\ 10^{-5}$
Soil density	ρ_s	$kg\,m^{-3}$	1410
Density of water	ρ_w	$kg\,m^{-3}$	1000
Soil moisture potential at saturation	Ψ_s	hPa	0.1717

Table 6. Parameters of maize for the three growth stages measured of De Sinderhoeve (Jacobs et al., 1990) used in tests

Parameter	Symbol	Unit	Value		
Maize height	H	m	2.20	2.30	2.20
Roughness length	z_0	m	0.114	0.114	0.114
Zero plane displacement	d	m	1.76	1.86	1.76
Leaf-area index	LAI	$m^2\,m^{-2}$	4.3	4.0	2.0
Fractional vegetation cover	σ_f		0.85	0.80	0.50
Minimum stomatal resistance	r_{smin}	$s\,m^{-1}$	200	200	200

that both of these schemes tend to overestimate the observations for the period considered, although this tendency is greater for LEAF. In contrast to them, LAPS's predictions of the latent heat flux agree quite well both in terms of trend and order of magnitude. Looking at panels of Fig. 1 and analyzing the period between 2000–2400 LST, it is evident that all schemes underestimate the measured latent heat fluxes. BATS and LAPS practically show the same behavior in terms of amount of predicted values while LEAF shows slightly smaller deviations from the observations. Generally, estimating the behavior of the schemes for the MA case for the whole period (noon–midnight), when the observed values of the surface fluxes were available, BATS and LAPS show good agreement with the observed values of the latent heat flux. However, LEAF shows a disagreement, with a tendency to predict higher latent heat flux values than actually occur. BATS and LAPS reproduce a correct trend in the period between noon and midnight, and they have values of the predicted sensible heat flux which are very close to each other. LEAF shows a similar behavior in the 1200–1400 LST and 2000–2400 LST intervals, respectively. However, between these intervals, LEAF constantly underestimates the measured values, having a very sharp drop in computed values between 1400 LST and 1500 LST. This reduction in the sensible heat is associated with the calculation of the net radiation rather than the parameterization of the sensible heat in the LEAF scheme. Namely, all three schemes use the net radiation to determine the canopy temperature, in turn a critical factor in calculation of sensible and latent heat flux. If we are looking in Fig. 1 at the behavior of the schemes over a diurnal period in the MA cases, it becomes apparent that there is a significant difference in the net radiation in the LEAF scheme and two others. The source of difference is primarily in the parameterization of the outgoing longwave component, depending on the longwave flux directed downward at the top of the canopy, vegetation fractional cover, canopy albedo, ground surface albedo, emissivities and temperatures of the ground surface and canopy, and its feedback with temperature of the canopy. Thus, the specification of the vegetation fractional cover σ_f and canopy albedo are both involved in determining these quantities and both can be greatly influenced, for example, by solar elevation angles (Vogel et al., 1995).

The MS case represents a situation when evapotranspiration also significantly prevails since the vegetation is still very dense ($\sigma_f = 0.80$,

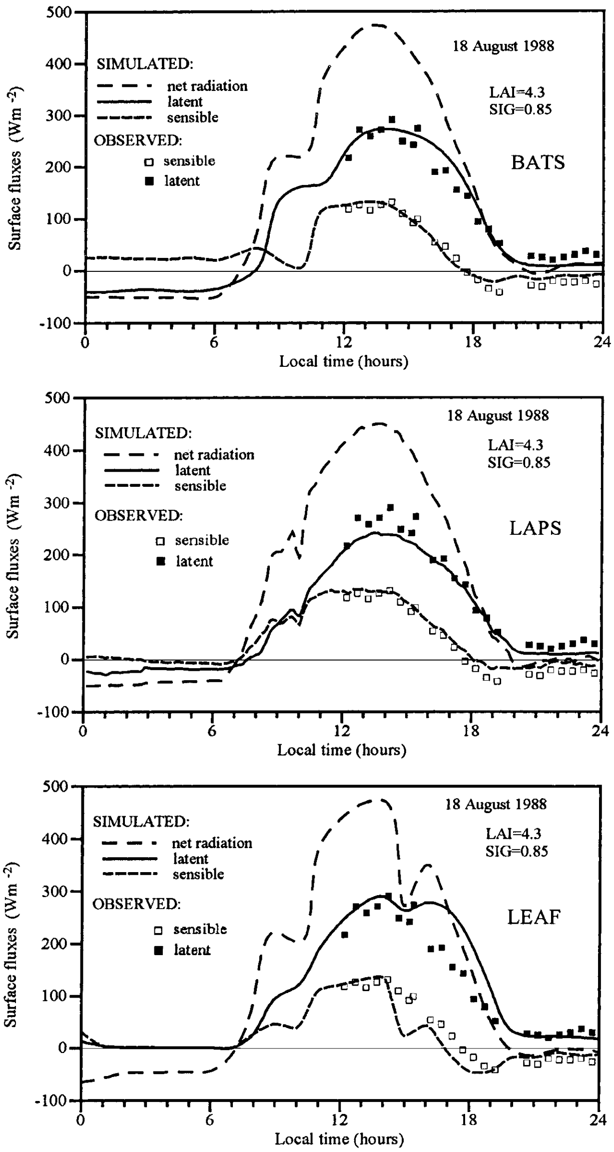

Fig. 1. Diurnal variations of simulated and observed surface fluxes above a maize canopy for 18 August 1988 at De Sinderhoeve (The Netherlands). The simulations were performed using all considered schemes. LAI and SIG denote leaf area index and fractional vegetation cover, respectively

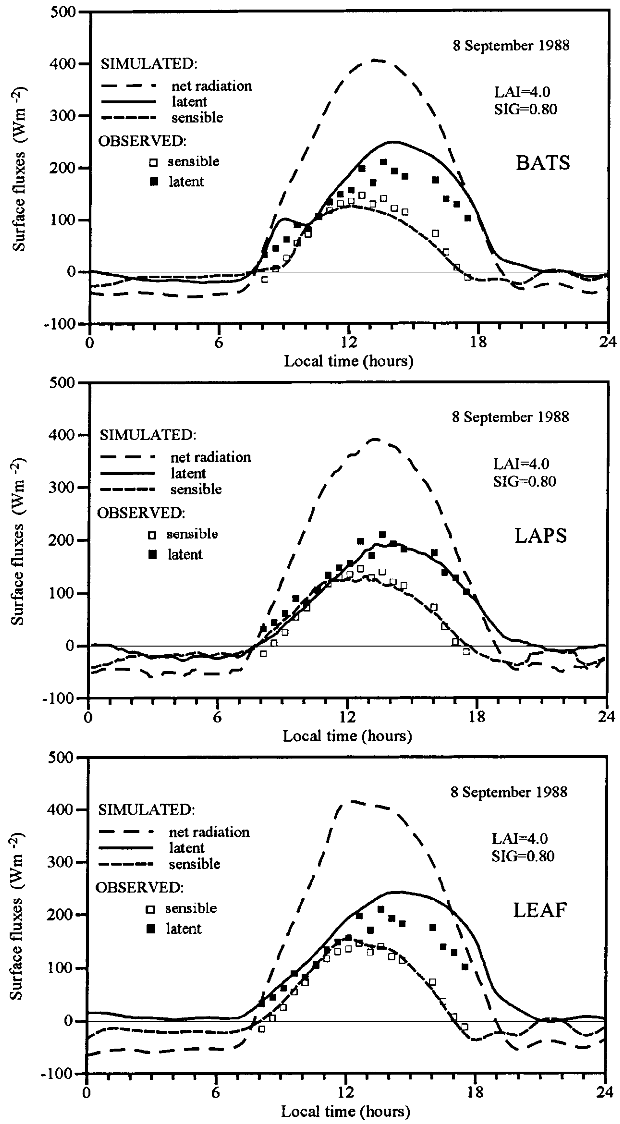

Fig. 2. As in Fig. 1 but for 8 September 1988

LAI = 4.0). Thus, the analysis of the schemes' behavior using this data set is useful for completing the discussion since we have available measured values for the period between early morning and noon which was not captured by the MA data set. The computed and the observed surface fluxes for the MS case are presented in Fig. 2. Apparently, the BATS and LEAF schemes retain the tendency to overestimate the measured latent heat fluxes, practically for the entire period (800–1700 LST). For both schemes this is much more evident for the afternoon. However, BATS overestimates the observations less than LEAF does. Generally, LAPS slightly underestimates the observed latent heat fluxes with more deviations for the period in the early morning. This behavior is expected and it coincides with the result obtained by the analysis of the MA case. Comparing all simulated diurnal variations of the latent heat fluxes we can conclude that LAPS has the best agreement. The trend of the sensible heat flux is modeled correctly by all schemes, including amounts of computed values. BATS has a very weak tendency toward underestimation but only around noon.

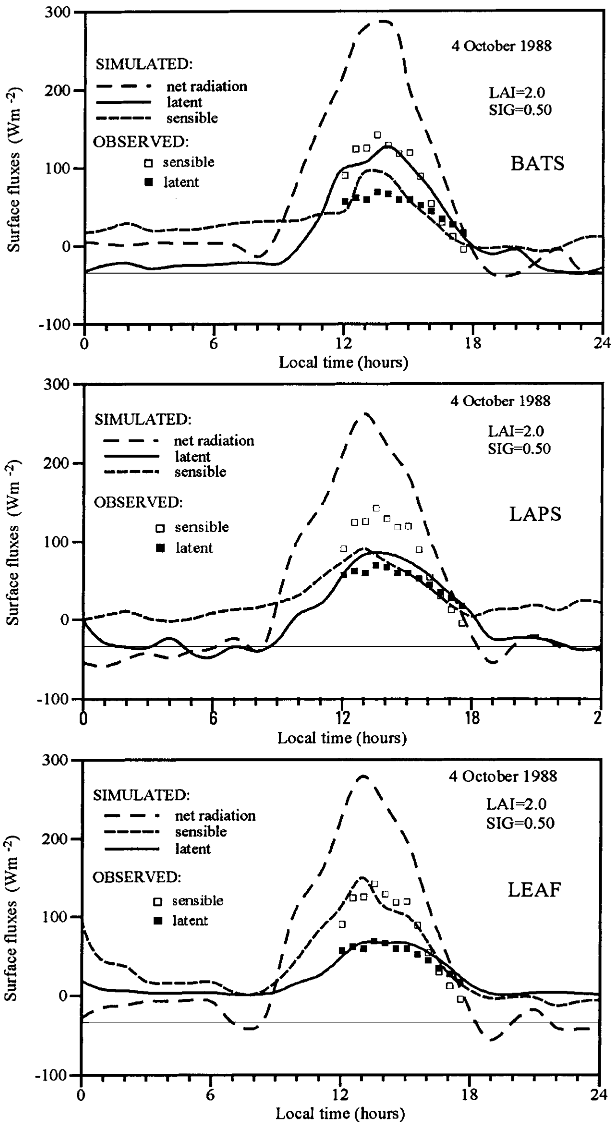

Fig. 3. As in Fig. 1 but for 4 October 1988

In the MO case, the vegetation fractional cover as well as the density of the maize canopy is significantly reduced ($\sigma_f = 0.50$, $\mathrm{LAI} = 2.0$) at the end of growing season, so the rate of evaporation was sharply decreased. Figure 3 shows surface flux outputs for all schemes obtained by running them using the MO data set. This situation is characterized by larger amounts of the sensible heat fluxes (vs. latent) because of the significant contributions from the bare soil fraction. It was a good opportunity for testing the scheme performances due to the partitioning of energy into sensible and latent heat parts. The best agreement in reproducing the latent heat course was achieved by LEAF. Next to this scheme is LAPS, with the simulated values, slightly overestimating the observations. The BATS scheme significantly overestimated the measured values, thus it gave the worst results. Obviously, in the presence of a larger fraction of bare soil, for example like the MO case, the corresponding evaporation scheme simulates evaporation in higher amounts than in the reality. However, this speculation needs more tests to be fully clarified. Similar results are obtained for the simulation of the sensible heat fluxes. Apparently, the best results are obtained by LEAF while BATS and LAPS calculated values which are much less than the observed ones.

In designing any land surface scheme, the problem of correct partitioning of the surface energy into sensible and latent heat fluxes is always present. Thus, any inacurate parameterization of the latent heat flux can seriously affect the Bowen ratio, i.e., the partitioning of energy between the latent and sensible heat at the surface, and, consequently, the accurate calculation of the ground and leaf temperature.

For example, Mihailović (1994) and Mihailović et al. (1995) showed the existence of large differences in the Bowen ratio and the predicted soil surface temperature when different formulations of the evaporation schemes are employed. According to Avissar and Pielke (1989) the correct parameterization of the Bowen ratio is of prime importance in assessing the quality of an atmospheric model and of the land surface scheme implemented within it. Consequently, comparison between the modeled and the observed Bowen ratio is a critical test for any land surface scheme. We have computed the Bowen ratio for all schemes and data sets. Results of the calculations are shown in Fig. 4. For the MA case, BATS and LAPS show quite good agreement for the period 1200–1800 LST. The LEAF shows some deviations after 1400 LST which coincides with the trend of the surface fluxes (Fig. 1). For the period indicated, the amount of the sensible heat flux goes down, thus the Bowen ratio decreases. Further, during the period between 1800 and 2400 LST, there is no agreement between the modeled values and the observations as achieved in the previous interval, regardless of the scheme used. (For the MS case, all schemes show a high level of agreement between the observed and computed values of the Bowen ratio

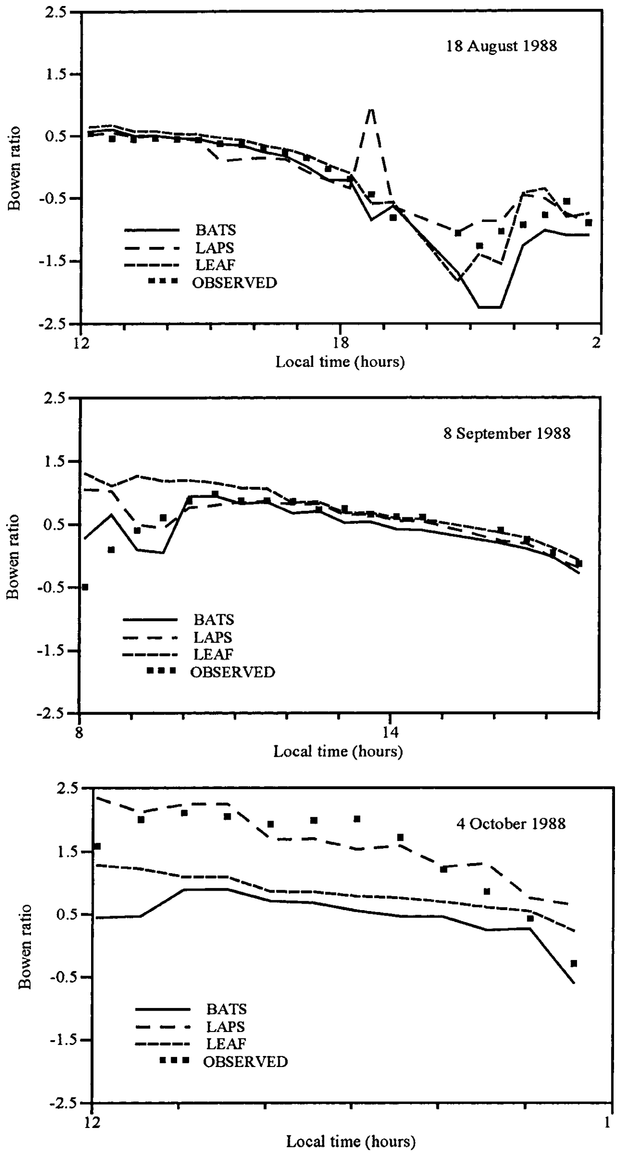

Fig. 4. Variations of simulated and observed Bowen ratio above a maize canopy for: 18 August (upper panel), 8 September (middle), and 4 October (lower panel). The simulations were performed using all considered schemes

for the 1000–1700 LST time interval). Finally, for the MO case, the Bowen ratio takes much larger values than in the previous cases because of the dominance of the sensible heat flux in the turbulent heat exchange. This fact is best followed by LEAF while smaller values of the Bowen ratio were achieved by LAPS and BATS.

The foregoing comparison of diurnal behavior of model results for each energy component with the observations will be supported by simple regression analysis and statistics.

Figure 5a–5c show the results of BATS, LEAF and LAPS schemes in computing the latent heat fluxes while Fig. 5d–5f illustrate the sensible heat fluxes obtained by the same schemes. Both groups of panels show the computed values plotted against the observations using all three data sets. It is seen that the LAPS scheme provides the best results with a tendency to underestimate the observations. In contrast to that, the BATS and LEAF mostly overestimate the observed values. The set of scatter plots for the sensible heat flux shows that the LEAF and LAPS have similar behavior, since both of them overestimate the measured fluxes. However, the BATS scheme mostly underestimates the observations.

In order to quantify the surface fluxes prediction we have performed an error analysis of model flux outputs, based on a method discussed in Pielke (1984) and later used by Mahfouf (1990). Following them we computed several statistical quantities as follows:

$$\nu = \left\{ \frac{1}{N} \sum_{i=1}^{N} (\Gamma_i - \hat{\Gamma}_i)^2 \right\}^{1/2} \tag{1}$$

$$\nu_{BR} = \left\{ \frac{1}{N} \sum_{i=1}^{N} [(\Gamma_i - \bar{\Gamma}) - (\hat{\Gamma}_i - \bar{\hat{\Gamma}})]^2 \right\}^{1/2} \tag{2}$$

$$\eta = \left\{ \frac{1}{N} \sum_{i=1}^{N} (\Gamma_i - \bar{\Gamma})^2 \right\}^{1/2} \tag{3}$$

and

$$\hat{\eta} = \left\{ \frac{1}{N} \sum_{i=1}^{N} (\hat{\Gamma}_i - \bar{\hat{\Gamma}})^2 \right\}^{1/2} . \tag{4}$$

Here Γ is the variable of interest (either latent or sensible heat flux in this study) while N is the total number of hourly data. An overbar indicates the arithmetic average, while a caret refers to an observation. The absence of a caret indicates a simulated value. ν is the root-mean-square (RMS) error, while ν_{BR} is a RMS error after a bias is removed. Root-mean-square errors give a good overview of a data set, with large errors weighted more than many small errors (Mahfouf 1990). The standard deviations in the predictions and in the observations are given by η and $\hat{\eta}$. A RMS which is less than the standard deviation of the observed field indicates skill in the prediction.

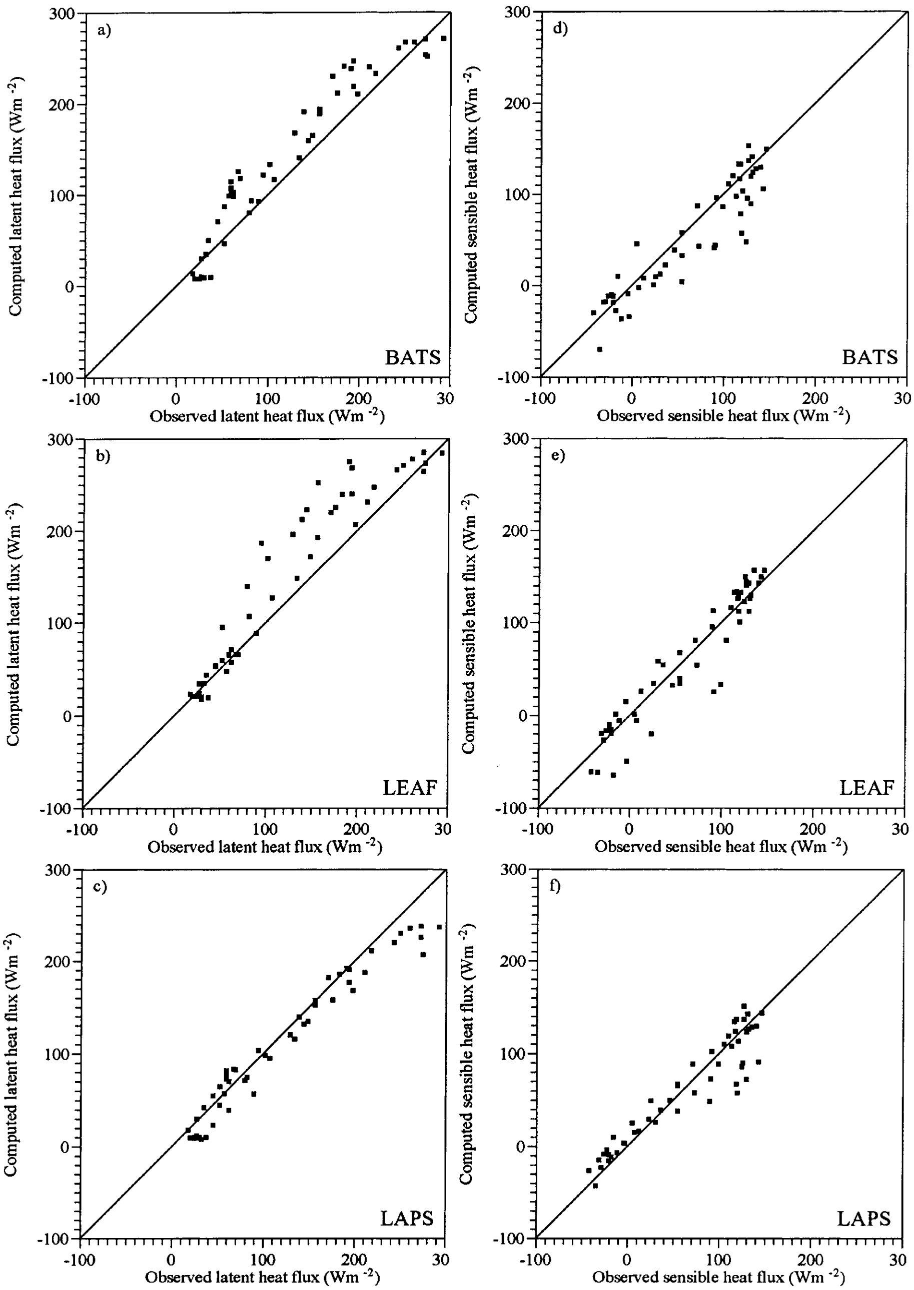

Fig. 5. Computed values of surface fluxes plotted against observations using results of simulations from Figs. 1–3 for: latent (5a–5c) and sensible (5d–5f) heat fluxes

Moreover, the values of η and $\hat{\eta}$ should be close if the prediction is to be considered realistic. The statistics for the latent and sensible heat fluxes are listed in Table 7. It indicates that the unbiased RMS for latent heat fluxes are: $31.4\,\mathrm{W\,m^{-2}}$, $20.6\,\mathrm{W\,m^{-2}}$ and $40.1\,\mathrm{W\,m^{-2}}$ for BATS, LAPS, and LEAF, respectively. These values were obtained when the statistical analysis was applied on a single data set obtained by a combination of all three available data sets. Survey of the unbiased RMS for sensible heat flux reveals that its values are very close for all schemes: $25.4\,\mathrm{W\,m^{-2}}$ (BATS), $21.5\,\mathrm{W\,m^{-2}}$ (LAPS) and $26.8\,\mathrm{W\,m^{-2}}$ (LEAF). A comparison of η and $\hat{\eta}$ shows that differences between them for the surface flux are smallest for LAPS and highest for LEAF. This analysis shows that the LAPS scheme slightly better simulates the surface fluxes than the two other schemes. The sources of these differences are very difficult to localize because they are not independent making the analysis more complicated.

Table 7. Error analysis of the land surface schemes predicted latent and sensible heat fluxes for the three data sets and the data set obtained by their unification

Heaf flux Statistical parameter according to Eqs. (1)–(4)	Latent W m^{-2}				Sensible W m^{-2}			
	ν	ν_{BR}	η	$\hat{\eta}$	ν	ν_{BR}	η	$\hat{\eta}$
Observation period (MA)								
BATS	21.7	21.7	110.1	101.3	15.9	15.5	69.8	65.1
LAPS	26.1	17.9	93.5	101.3	13.5	8.9	65.3	65.1
LEAF	45.8	37.1	112.0	101.3	28.2	26.5	71.4	65.1
Observation period (MS)								
BATS	34.7	18.4	63.7	52.4	21.1	20.5	57.1	55.1
LAPS	16.8	11.8	57.0	52.4	13.0	11.8	48.4	55.1
LEAF	45.3	21.3	56.5	52.4	30.2	25.8	57.1	55.1
Observation period (MS)								
BATS	39.9	19.4	34.8	15.7	40.8	20.8	35.0	48.3
LAPS	13.0	6.9	20.8	15.7	37.6	23.3	28.0	48.3
LEAF	7.0	5.8	13.6	15.7	17.0	15.0	41.6	48.3
All data sets								
BATS	31.4	25.1	87.2	82.1	25.4	23.8	60.7	62.4
LAPS	20.6	18.2	74.7	82.1	21.5	21.5	55.4	62.4
LEAF	40.1	30.6	94.0	82.1	26.8	26.6	69.3	62.4

The main source of possible differences in calculating the surface fluxes in these schemes lies in combination of errors associated with determining the canopy temperature and errors produced in assuming that the eddy diffusivities of heat and momentum are equal. Namely, in simple resistance-analog equation utilized for calculating the sensible heat flux (LAPS and LEAF, Table 2c), the two primary assumptions are often made. First, numerical modelers assume that the aerodynamic resistance for sensible heat flux is equivalent to that for momentum. Second, the infrared canopy temperature measurements are assumed to be the surface temperature of the vegetation elements. Thus, Baldocchi (1994) showed that 1 °C difference between these two temperatures can cause 30–60 W m^{-2} errors in calculating the sensible heat flux. On the other hand, BATS based on Deardorff's concept (Deardorff, 1978) determines the canopy temperature from a foliage surface energy budget equations and performs reasonably well (Vogel et al., 1995). According to this author this concept in parameterization gives good results in sensible heat calculations. However, in the tests LAPS, also, gives comparable results for sensible heat, although it is based on another concept.

Panels in Fig. 6 show the observed values of leaf temperature and its diurnal variations modeled by BATS, LAPS, and LEAF, corresponding to the three considered data sets. First, looking at the upper panel, representing the MA case, the behavior of the leaf temperature predicted by all schemes follows the trend exhibited by observations during the period when data were available. In this period, the calculated values of the canopy temperature mostly comparable with observations. However, a detailed survey of the drawn curves indicates slight differences between the schemes in predicting leaf temperature. In the 1200–1500 LST period, LAPS overestimates the observed leaf temperatures much more than BATS does. LEAF follows observations quite well except for the 1400–1500 LST time interval when some underestimation in predicted temperature occurred. A possible explanation for these differences could be considered in terms of various amounts of water evaporated from leaves (latent heat fluxes) predicted by schemes (Fig. 1). Thus, in the period indicated, LAPS predicts latent heat flux in amounts which are smaller than the observed latent heat fluxes coming from the active surface of the maize canopy. Consequently, the canopy temperatures simulated by LAPS becomes higher than their measured values. In the late afternoon, LEAF predicts lower temperatures than observed since the latent heat fluxes predicted by this scheme are higher than their actual

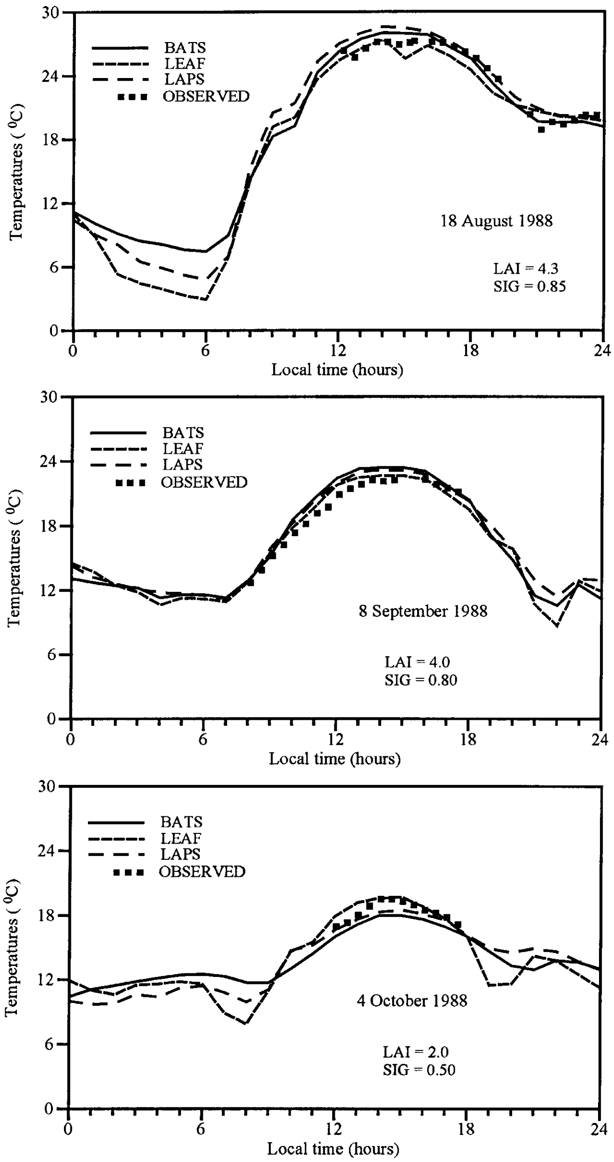

Fig. 6. Diurnal variations of simulated and observed canopy temperatures for three situations at De Sinderhoeve (The Netherlands). The simulations were performed using all considered schemes. LAI and SIG denote leaf area index and fractional vegetation cover, respectively

values in this part of the diurnal cycle, when the BATS and the LAPS simulations of canopy temperature follow observation much better. Finally, the time interval between 000 LST and 800 LST is interesting for comparison although there were no available observations to validate the models. There are evident differences between canopy temperatures predicted in this interval. After midnight, these differences increase; thus around 600 LST they reach a maximum of 5 °C (between the BATS and the LEAF).

Concerning the MS case, all schemes appear to operate realistically with an overestimation in the period between 800 LST and 1400 LST. Good simulations of the leaf temperature for the MO case were obtained by LEAF and partly by LAPS while BATS gives temperatures which underestimate the observed values.

5. Concluding remarks

Three land surface parameterization schemes designed for different purposes were compared over a daily time scale using three data sets obtained above a maize field at De Sinderhoeve (The Netherlands). On the basis of the results obtained with the data sets, available observations and the corresponding discussion we can summarize the conclusions as follows. All schemes correctly predict values of the latent heat flux. More deviations from the observations, with the tendency to overestimate, were found for BATS for the MO case (when LEAF gives the best results) and for LEAF in the MA and MS case, respectively. A similar behavior was partly found for the LAPS scheme for the MA case when it underestimates the measured values. Generally, LAPS and BATS simulate evaporation well while its simulation by LEAF differs slightly more from the observations than is achieved by the two other schemes. Concerning the sensible heaf flux, each scheme simulates it well for the MA and MS case. However, LEAF had the best agreement for the MO case.

There are no significant differences between compared schemes in predicting the canopy temperature. The only exception is the MO case when BATS and LAPS produce some values which are in disagreement with the observed ones.

Evidently, there are some differences in surface fluxes and canopy temperature predictions among the considered schemes. However, there is no definite conclusion about the superiority of any of those schemes. In order to obtain that conclusion, we need more specific tests, for example, with long term integrations including intensive tests with soil moisture prediction such as being conducted by PILPS (Shao et al., 1995). This study does, however, define an expected level of uncertainty associated with these land-atmosphere interaction models.

Acknowledgments

The authors thank Addo van Pul for supplying the experimental data for maize while the first author spent four months at the Wageningen Agricultural University as a visiting scientist. We would also like to thank Dallas McDonald for patiently preparing and editing this paper. This work is supported by the U.S.-Yugoslav Board under NSF Grant No. 993/1991, NSF Grant No. ATM-9306754, and the Federal Ministry for Development, Science and Environment of Republic Yugoslavia 2/0 10. No. 032 94-1.

References

Avissar R, Pielke RA (1989) A parameterization of heterogeneous land surface for atmospheric numerical models and its impact on regional meteorology. Mon Wea Rev 117: 2113–2136

Baldocchi DD (1992) A lagrangian random-walk model for simulating water vapor, CO_2, and sensible heat flux densities and solar profiles over and within a soybean canopy. Bound-Layer Meteorol 61: 113–144

Betts AK, Chen F, Mitchell KE, Janjić Z (1997) Assessment of the land surface and boundary layer models in two operational versions of the NCEP Eta using FIFE data. Mon Wea Rev 125: 2896–2916

Chen F, Janjić Z, Mitchell K (1997) Impact of atmospheric surface-layer parameterization in the new land-surface scheme of the NCEP mesoscale Eta model. Bound-Layer Meteorol 85: 391–421

Chen TH, Henderson-Sellers A, Pitman AJ, Shao Y, Boone A, Chen F, Desborough CA, Dickinson RE, Ek MB, Garratt JR, Gedney N, Gusev YM, Koster R, Kowalczyk E, Laval K, Lean J, Lettenlaier D, Liang X, Mahfouf JF, Schulz JP, Shmakin AB, Verseghy DL, Wetzel P, Wood EF, Xue Y, Yang ZL (1997) Cabauw experimental results from the project for intercomparison of land-surface parameterization schemes. J Climate 10: 1194–1215

Deardorff JW (1978) Efficient prediction of ground surface temperature and moisture, with inclusion of a layer of vegetation. J Geophys Res 83: 1889–1903

Dickinson RE, Henderson-Sellers A, Kennedy PJ, Wilson MF (1986) Biosphere-Atmosphere Transfer Scheme (BATS) for the NCAR Community Climate Model, NCAR Tech. Note, NCAR, TN275+STR, 69 pp

Dickinson RE, Henderson-Sellers A, Kennedy PJ, Giorgi F (1992) Biosphere-Atmosphere Transfer Scheme (BATS). Version 1e as a coupled to the NCAR Community Climate Model, NCAR Tech Note

Henderson-Sellers A, Yang ZL, Dickinson RE (1993) The project for intercomparison of land-surface parameterization schemes. Bull Amer Meteor Soc 74: 1335–1349

Jacobs AFG, van Pul WAJ, van Dijken A (1990) Similarity moisture dew profiles within a corn canopy. J Appl Meteor 29: 1300–1306

Lee TJ (1992) The impact of vegetation on the atmospheric boundary layer and convective storms. Ph. D. Dissertation, Colorado State University, Department of Atmospheric Science, Fort Collins, Colorado, 137 pp

Lohmann D, Nolte-Holube R, Raschke E (1996) A large horizontal routing to be coupled to land surface parameterization schemes. Tellus 48A: 706–721

Mahfouf JF (1990) A numerical solution of the surface water budget during HAPEX MOBILHY. Bound-Layer Meteorol 53: 201–222

Manabe S (1969) Climate and ocean circulation: 1, The atmospheric circulation and the hydrology of the earth's surface. Mon Wea Rev 97: 739–805

Mihailović DT (1990) Testing the Biosphere-Atmosphere Transfer scheme (BATS) using Penman and Long (1960) data: Preliminary results. Internal Report. Department of Meteorology, Wageningen Agricultural University, 6071 AP Wageningen. The Netherlands, 40 pp

Mihailović DT (1996) Description of a land-air parameterization scheme (LAPS). Special Issue of Global & Planetary change on Soil Moisture Simulation 13:207–215

Mihailović DT, Rajković B (1994) Impact of differently designed bare soil evaporation schemes on variability of Bowen ratio and ground temperature in land-air parameterization modelling. Meteor Z 3: 312–318

Mihailović DT, Ruml M (1996) Design of land-air parameterization scheme (LAPS) for modelling boundary layer surface processes. Meteorol Atmos Phys 58: 65–81

Mihailović DT, Kallos G (1997) A sensitivity study of a coupled-vegetation boundary layer scheme for use in atmospheric modelling. Bound-Layer Meteorol 82: 283–315

Mihailović DT, Lalić B, Arsenić ID (1997) The main features of the hydrological module in the Land Air Parameterization Scheme (LAPS). Phys Chem Earth 21(3): 201–204

Mihailović DT, de Bruin HAR, Jeftić M, van Dijken A (1992) A study of land surface parameterizations to the inclusion of different fractional covers and soil textures. J Appl Meteor 31: 1477–1487

Mihailović DT, Kallos G, Lalić B, Papadopoulos A, Arsenić I (1999) Parameterization of hydrological processes for application to regional and mesoscale modeling. Global Atmosphere and Ocean System 7: 73–89

Mihailović DT, Pielke RA, Rajković B, Lee TJ, Jeftić M (1993) A resistance representation of schemes for evaporation from bare and partly plant-covered surfaces for use in atmospheric models. J Appl Meteor 32: 1038–1054

Mihailović DT, Rajković B, Lalić B, Jović D, Dekić Lj (1998) Partitioning the land surface water simulated by a land-air surface scheme. Journal of Hydrology 211: 17–33

Mihailović DT, Rajković B, Lalić B, Dekić Lj (1995) Schemes for parameterizing evaporation from non-plant covered surface and their impact on partitioning the surface energy in land-air exchange parameterization. J Appl Meteor 34:2462–2475

Pielke PA (1984) Mesoscale meteorological modelling. New York: Academic Press, 612 pp

Shao Y, Rama AD, Henderson-Sellers A, Thornton P, Liang X, Chen TH, Ciret C, Desborough C, Balachova O, Haxeltine A, Ducharne A (1995) Soil moisture simula-

tion. A report of the RICE and PILPS Workshop. IGPO Publication Series, Washington, No. 14, p. 179
van Pul WAJ (1992) The flux of ozone to a maize crop and the underlying growing season. Ph.D. Thesis, Wageningen Agricultural University, 147 pp
Vogel CA, Baldocchi D, Luhar AK, Rao KS (1995) A comparison of a hierarchy of models for determining energy balance components over vegetation canopies. J Appl Meteor 34: 2182–2196

Authors' addresses: D.T. Mahailović, B. Lalić, I.D. Arsenić, Faculty of Agriculture, University of Novi Sad, 21000 Novi Sad, Yugoslavia; T.J. Lee, Science Applications International Inc., McLean, VA 22102, U.S.A.; R.A. Pielke, Department of Atmospheric Science, Colorado State University, Fort Collins, CO 80523, U.S.A.; B. Rajković, Faculty of Physics, University of Belgrade, 11000 Belgrade, Yugoslavia; P.L. Vidale, Klimaforschung ETH/Climate Research ETH, Zurich, Switzerland.